# Mechanical Activation of a Multimeric Adhesive Protein Through Domain Conformational Change

Sithara S. Wijeratne,[1] Eric Botello,[1] Hui-Chun Yeh,[2] Zhou Zhou,[3] Angela L. Bergeron,[2] Eric W. Frey,[1] Jay M. Patel,[1] Leticia Nolasco,[4] Nancy A. Turner,[4] Joel L. Moake,[4] Jing-fei Dong,[3,5,*] and Ching-Hwa Kiang[1,4,†]

[1]*Department of Physics and Astronomy, Rice University, Houston, Texas 77005, USA*
[2]*Department of Medicine, Thrombosis Division, Section of Cardiovascular Sciences, Baylor College of Medicine, Houston, Texas 77005, USA*
[3]*Puget Sound Blood Center, Seattle, Washington 98104, USA*
[4]*Department of Bioengineering, Rice University, Houston, Texas 77005, USA*
[5]*Department of Medicine, Division of Hematology, University of Washington, Seattle, Washington 98104, USA*

(Received 6 July 2012; revised manuscript received 21 December 2012; published 5 March 2013)

The mechanical force-induced activation of the adhesive protein von Willebrand factor (VWF), which experiences high hydrodynamic forces, is essential in initiating platelet adhesion. The importance of the mechanical force-induced functional change is manifested in the multimeric VWF's crucial role in blood coagulation, when high fluid shear stress activates plasma VWF (PVWF) multimers to bind platelets. Here, we showed that a pathological level of high shear stress exposure of PVWF multimers results in domain conformational changes, and the subsequent shifts in the unfolding force allow us to use force as a marker to track the dynamic states of the multimeric VWF. We found that shear-activated PVWF multimers are more resistant to mechanical unfolding than nonsheared PVWF multimers, as indicated in the higher peak unfolding force. These results provide insight into the mechanism of shear-induced activation of PVWF multimers.

DOI: 10.1103/PhysRevLett.110.108102 PACS numbers: 87.14.E−, 82.37.Gk, 82.37.Rs

The von Willebrand factor (VWF) is a large multimeric protein constructed from two identical VWF monomers linked by *C*-terminal disulfide bonds into dimers, and the dimers then polymerize via *N*-terminal disulfide bonds into long VWF multimers [1–3]. The domain organization of a 250 kDa, 60 nm long VWF monomer [2,4] is shown in Fig. 1(a). The largest VWF multimers contain up to 200 monomers [5] and are concentrated after synthesis in Weibel-Palade bodies and $\alpha$ granules, the storage compartments of endothelial cells and platelets, respectively [2]. In response to stimulation by cytokines and other agents, these ultralarge VWF (ULVWF) multimers are rapidly secreted in long stringlike structures by endothelial cells, where they are anchored [6]. Endothelial cell-anchored ULVWF multimeric strings are hyperadhesive in their capacity to bind platelet glycoprotein (GP) Ib-IX-V complexes [3,7]. Circulating PVWF multimers are hemostatically inactive toward platelets but can be activated by exposure to high shear stress [2,8,9]. It has been proposed that, under high shear stress, PVWF multimers undergo a change in conformation from a globular to an elongated form (quaternary structure change) [2,9–11]. More recently, it has been demonstrated that shear-activated PVWF multimers become laterally apposed into fibrils via multimer-to-multimer disulfide bonds [12].

The shear-induced conformational change exposes or alters the A1 domain in VWF monomeric subunits, enabling large VWF multimers to bind to platelet GP Ib-IX-V and to initiate platelet adhesion and aggregation. The difference in the dynamic states of various forms of VWF multimers determines the on-off switching of VWF multimeric activation for platelet binding. In this study, we used single-molecule manipulation to monitor the force response of different forms of VWF multimers. The peak force was used as an indicator of the dynamic states of VWF monomeric subunit domains within VWF multimers.

We pulled single VWF multimeric molecules using an atomic force microscope (AFM) [Fig. 1(b)] (see the Supplemental Material [13]). The sawtooth patterns of force peaks in the force-extension curves of PVWF multimers [Figs. 1(c) and 1(d)] are characteristic of multidomain protein unfolding (tertiary structure change) [14–16]. The value of the peaks specifies the force required to unfold the domains and is related linearly to the unfolding free energy barrier and logarithmically to the pulling speed [Fig. 2(a)] [16–18]. The change in the contour length ($\Delta L_c$) histogram of the PVWF [Fig. 2(b)] shows a major peak at 30(8) nm. The values in the parentheses are 1 standard deviation. This is a typical length for an unfolded domain of 85 amino acid residues, assuming 0.36 nm per residue [5,19]. In addition, there was a minor peak at 60(15) nm, corresponding to an unfolded domain of 170 amino acid residues, consistent with domain unfolding.

ULVWF multimers contain a larger number of monomers than PVWF multimers and are more active in adhering to platelets and inducing platelet aggregation [20]. We observed differences in peak unfolding forces at high pulling speeds between ULVWF and PVWF multimers

 

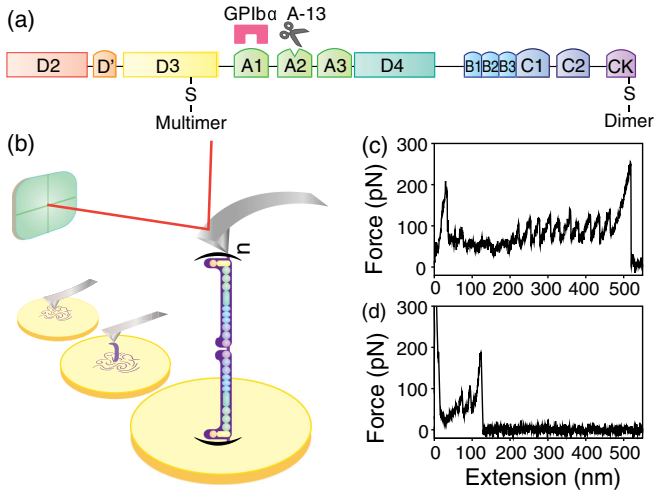


FIG. 1 (color online). Multimeric VWF unfolding with AFM. (a) The domain organization of a VWF monomeric subunit, where A1 is the platelet GP Ib-IX-V receptor-binding domain, A2 contains the cleavage site for ADAMTS-13, and A3 contains the binding site for the subendothelial matrix collagen. The locations of the disulfide bonds where the VWF connects to form dimers and multimers are presented. (b) Experimental setup of the single-molecule pulling of a VWF multimer using AFM. A purified PVWF multimer, which is composed of $n$ polymerized dimers of a VWF, was pulled while the force was recorded. Typical force-extension curve of (c) a PVWF multimer and (d) a PVWF dimer, pulled at a constant velocity of 1000 nm/s.

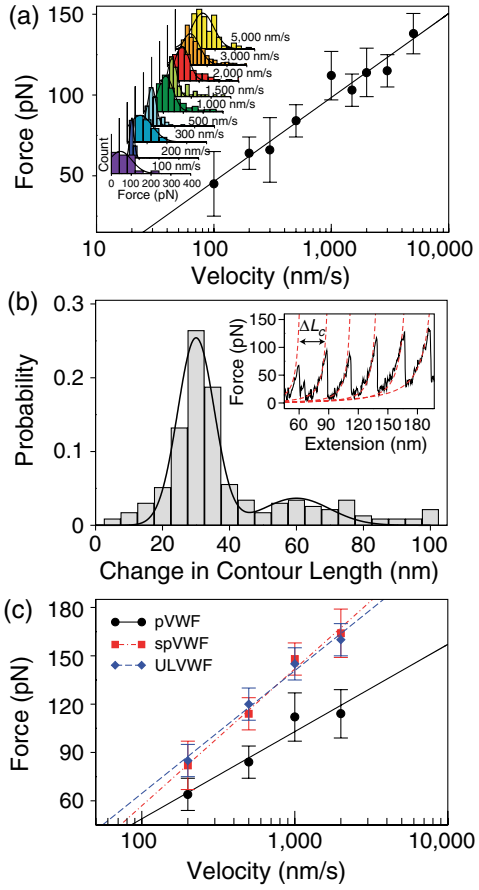


FIG. 2 (color online). Unfolding of a multimeric VWF. (a) Unfolding force as a function of pulling velocity for a PVWF. The unfolding forces were binned by pulling velocity. The inset shows the binned histograms fitted with Gaussian curves. The peak of the fitted Gaussian was plotted against the pulling velocity. The error bars indicate half-bin width. The line is a linear fit to the logarithm of the velocity. (b) Histogram of the change in contour length of the PVWF. The solid line indicates a double Gaussian fit to the distribution, which has a major peak at 30 nm and a minor peak at 60 nm. We analyzed all the data together, and therefore the major contribution of the data comes from $\Delta L_c$ 30 nm. Inset: the change in contour length, $\Delta L_c$, was the difference of the $L_c$ determined by the wormlike chain model fit to the data (dashed red lines), $F(x) = \frac{k_B T}{L_p}[\frac{1}{4(1-x/L_c)^2} - \frac{1}{4} + \frac{x}{L_c}]$, where $F$ is the force; $x$ is the distance; $L_p$ and $L_c$ are the persistence length and the contour length, respectively; $T$ is the temperature; and $k_B$ is the Boltzmann constant [33–35]. The persistence length $L_p$ was 0.4 nm, which is consistent with unfolded protein chains. (c) Velocity-dependent unfolding forces of different forms of multimeric VWFs. The trend is similar to protein domain unfolding.

[Fig. 2(c)], indicating that PVWF and ULVWF multimers are in different conformational states. Similarly, at high levels of shear stress (60–120 dyn/cm$^2$), the capacity of PVWF multimers to adhere to and aggregate to platelets increases, as previously shown [20] and re-affirmed in this study (see Supplemental Fig. 1 [13]). That is, shear-activated PVWF (SPVWF) multimers become functionally similar to ULVWF multimers. The peak unfolding force of PVWF multimers increased after exposure to high shear stress, but the force-extension curves are qualitatively similar to unsheared PVWF multimers and unsheared ULVWF multimers. However, the reaction of PVWFs to SPVWFs may not be 100%, and the shift in the peak force is a qualitative observation. The difference in the peak unfolding forces between PVWF multimers and either SPVWF or ULVWF multimers was more pronounced at high pulling velocities [Fig. 2(c)]. This finding is compatible with the shear-induced conformational change in the PVWF (to the SPVWF) that increases the exposure of platelet-binding A1 domains in the VWF monomeric subunits of the SPVWF multimers. It has been shown that exposure to a 100 dyn/cm$^2$ high fluid shear stress induces PVWF multimers to associate laterally and form VWF fibrils that have an increased capacity to bind to platelet GPIb$\alpha$ [8]. This fibrillar state of laterally associated VWF multimers may be the conformation of SPVWF multimers that is functionally similar to the ULVWF (see Supplemental Fig. 2 [13]).

To measure the kinetics in SPVWF force experiments, peak unfolding force measurements of the PVWF were conducted at different delay times after shear exposure. The SPVWF unfolding force decreased over time and reached an equilibrium force after 10 h [Figs. 3(a) and 3(b)]. Thus, the shear-induced change in the PVWF to the SPVWF

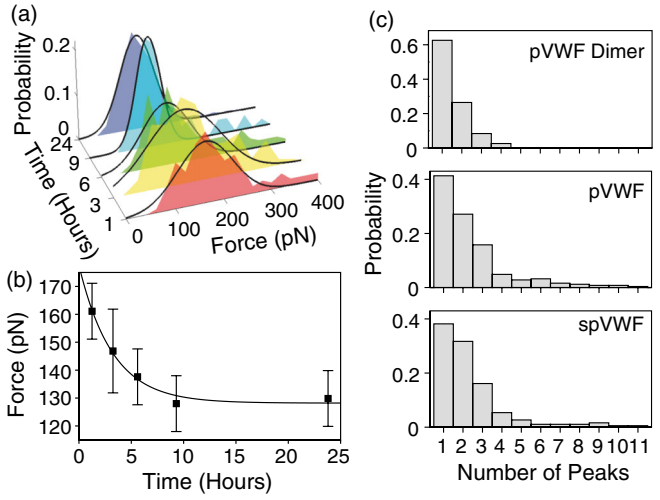


FIG. 3 (color online). Dynamics of VWF multimers. The data were taken at a 1000 nm/s pulling velocity. (a) Peak force distributions of the SPVWF as a function of time since exposure to a pathological level of 100 dyn/cm$^2$ fluid shear. (b) The SPVWF peak force decreases with time since shear exposure. The solid line is a fit to an exponential curve, $F(t) = F_p + (F_s - F_p)\exp(-t/\tau)$ (see the text). The error bars are half of the bin width in the histogram. (c) Number of unfolding peaks in a given force curve from different forms of VWF multimers. The PVWF dimer has up to four force peaks, indicating that there are two unfolding events per monomer.

multimeric conformation changes with time, with a prolonged relaxation time of several hours. Fitting the data to the exponential equation $F(t) = F_p + (F_s - F_p) \times \exp(-t/\tau)$, where $F_s$ is the peak force immediately after shear exposure, $F_p$ is the equilibrium peak force, and $\tau$ is the time constant, yields $F_s = 180$ pN, $F_p = 130$ pN, and $\tau = 3$ h.

The force-extension curves showed that the unfolding force peaks correspond to the changes in the VWF multimeric conformation at the level of one or more domains within the VWF monomeric subunits. This conclusion is supported by three factors: (i) the force-extension curves display a characteristic sawtooth pattern of repeated force peaks, resembling the known sequential unfolding of other multidomain proteins [14], (ii) the increase in contour length after each peak, $\Delta L_c$, is 30 nm, which is comparable to the contour length of an unfolded domain or an intermediate state, and (iii) at 1000 nm/s pulling velocity, the value of the peak unfolding force was distributed at 100–130 pN and varied linearly with the natural logarithm of the pulling velocity, as is typical of domain unfolding.

In addition, by stretching VWF dimers under similar conditions, we have observed up to four unfolding peaks per force-extension curve [Fig. 3(c)], suggesting that there are two unfolding events per monomer. The two force peaks can be from the unfolding of two different domains or from two partial domains. This conclusion is supported because, when pulling eight serially linked titin I27 domains, $(I27)_8$, up to eight unfolding peaks have been observed [14]. For comparison, PVWF curves have up to ten force peaks, suggesting that there are up to five monomers at a given pull. The number of peaks of the ULVWF does not differ from the PVWF or SPVWF significantly, even though the ULVWF sample has more repeating units than the PVWF [13]. Hence, it suggests a stronger interaction in the ULVWF among monomers that may prevent the ULVWF polymer chain from being isolated in order to undergo domain unfolding. The dimer force peak and change in contour length, $\Delta L_c$, distributions are consistent with that of the multimer, further supporting the conclusion that the features in the multimeric VWF force-extension curves correspond to individual domain unfolding.

In the monomeric subunits of VWF multimers, the force peaks may be the combined result of the unfolding of different domains. It is likely, however, that there is a major contributor to the force signal. A probable candidate is the VWF A2 domain because it does not have disulfide bonds and has been observed to unfold in the pN force range [21,22]. $\Delta L_c$ of 60(15) nm determined from our experiment is similar to 57(5) nm observed by Zhang *et al.* [5]. The most frequent $\Delta L_c$ observed, 30(8) nm, is consistent with the values reported by Zhang *et al.* [5], showing 40% of the unfolding peaks with $\Delta L_c$ of 23(5) nm, which is attributed to the partial unfolding of A2 [5,21,23]. The A1 and A3 domains contain disulfide bonds, which are unlikely to unfold during stretching experiments because, at a 100 nm/s pulling velocity, disulfide bonds typically rupture at 2 nN [24], a force much higher than the typical unfolding force (100–200 pN) observed in our study. Previous studies of the forced unfolding of A1A2A3 triple domains also reveal that the VWF A2 domain can be partially or completely unfolded, possibly after interdomain uncoupling [23,25]. These findings suggest that the unfolding of a portion of the A2 domain in VWF monomeric subunits may be the main contributor to our unfolding force signals. We have ruled out that the change of unfolding force is simply due to more exposed A2 domains without intramolecular interactions, since such a configuration will only yield more unfolding peaks in a given pull [Fig. 3(c)] but not a significantly altered unfolding force [10,17].

Our results suggest that high shear stress (100 dyn/cm$^2$) converts SPVWF multimers to a conformation that was metastable, probably due to the lateral association of SPVWF multimers, with a long relaxation time. Over several hours, the metastable state of SPVWF crossed the energy barrier and relaxed to a more stable state. Using the time constant $\tau = 3$ h determined from the relaxation curve shown in Fig. 3(b), we estimated the activation free energy barrier from the SPVWF to the PVWF, using the Arrhenius equation, $k = A\exp(-\Delta G/k_B T)$, where $k = 1/\tau$ is the rate constant, $\Delta G$ is the free energy of the barrier from the SPVWF to the PVWF, and $A$ is the

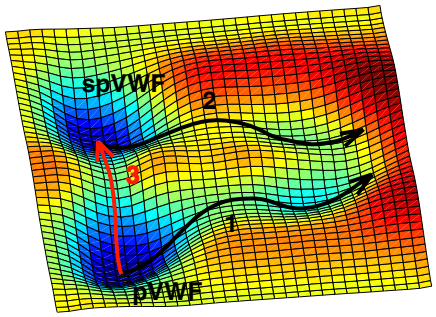


FIG. 4 (color online). Free energy landscape of the multimeric VWF. The PVWF is the native equilibrium state. Fast stretching of PVWF molecules results in domain unfolding (pathway 1), while the SPVWF domain unfolds through a different pathway (pathway 2). High shear stress promotes the PVWF to the metastable SPVWF state (pathway 3), which relaxes to a lower energy state, over several hours. The barriers of pathways 1 and 2 result in the force peaks observed for the PVWF and the SPVWF, respectively. The barrier of pathway 3 contributes to the change in peak force in the time-dependent studies of SPVWF shown in Fig. 3(b).

preexponential factor. Assuming that $A$ is between $10^5$ and $10^{10}$ $s^{-1}$, $\Delta G$ is 12–19 kcal/mol [26–28]. The barrier height from an active state to an inactive state is comparable to protein unfolding, further supporting the notion of domain conformational changes for the observed force peak change.

Figure 4 highlights the free energy landscape [29] of different forms of VWF multimers. Our results suggest that PVWF multimers have different conformational states before and after shear exposure that unfold through different pathways (pathways 1 and 2). Proteins with multiple conformational states of different activities have been observed by force measurements [30]. Here, PVWF multimers are in a native inactive state but can be converted to a metastable active state (SPVWF) by exposure to high shear stress. This state may be considered ''misfolded'' since it is a non-native state [31]. The SPVWF multimer's peak unfolding force, which is related to the barrier height [17,32], is likely to be higher than that of PVWF multimers because high shear stress induces the lateral association of several PVWF multimers into a fibrillar form with SPVWF multimers. Thus, shear effects on VWF monomeric A2 domains cause an associated increase in the exposure of platelet-binding VWF A1 domains.

In summary, our results demonstrate that PVWF multimers have a different conformational state that unfolds via a different pathway after exposure to high shear stress. The PVWF is in a native inactive state that can be converted to a metastable active state, the SPVWF, by high shear stress. The peak unfolding force of SPVWF multimers is higher than that of unsheared PVWF multimers, potentially because high shear stress induces the lateral association of PVWF multimers into a fibrillar form, as indicated by the formation of large VWF aggregates after shear exposure. Thus, an increased intramolecular interaction shifts the domains to a different state that has a higher unfolding barrier. Shear-activated conformational changes in the A2 domains in VWF monomeric subunits of SPVWF multimers may provoke an increased exposure of neighboring (platelet-binding) A1 domains. The effect decreases over several hours. It will be interesting to investigate if structural studies can resolve the two states and what external factors, whether physical, chemical, or biological, may affect the stability of and switching rate between these states.

We acknowledge NIH Grants No. HL71895 and No. HL85769 (J.-F. D.), NSF Grant No. 0907676, NIH Grant No. GM008362, and Welch Foundation Grant No. C-1632 (C.-H. K.); the ANH (DOE/NASA) and NIGTP NIH Grant No. T32EB009379 (E. W. F.); and the Mary R. Gibson Foundation and the Everett Hinkson Fund (J. L. M.) for support.

*jfdong@psbc.org
†chkiang@rice.edu

[1] Z. M. Ruggeri, Curr. Opin. Hematol. **10**, 142 (2003).
[2] J. E. Sadler, Annu. Rev. Biochem. **67**, 395 (1998).
[3] J. L. Moake, C. K. Rudy, J. H. Troll, M. J. Weinstein, N. M. Colannino, J. Azocar, R. H. Seder, S. L. Hong, and D. Deykin, N. Engl. J. Med. **307**, 1432 (1982).
[4] W. E. Fowler, L. J. Fretto, K. K. Hamilton, H. P. Erickson, and P. A. McKee, J. Clin. Invest. **76**, 1491 (1985).
[5] X. Zhang, K. Halvorsen, C.-Z. Zhang, W. P. Wong, and T. A. Springer, Science **324**, 1330 (2009).
[6] Y. Li, H. Choi, Z. Zhou, L. Nolasco, H. J. Pownall, J. Voorberg, J. L. Moake, and J.-F. Dong, J. Thromb. Haemost. **6**, 1135 (2008).
[7] J.-F. Dong, J. L. Moake, L. Nolasco, A. Bernardo, W. Arceneaux, C. N. Shrimpton, A. J. Schade, L. V. McIntire, K. Fujikawa, and J. A. López, Blood **100**, 4033 (2002).
[8] H. Choi, K. Aboulfatova, H. J. Pownall, R. Cook, and J.-F. Dong, J. Biol. Chem. **282**, 35 604 (2007).
[9] S. W. Schneider, S. Nuschele, A. Wixforth, C. Gorzelanny, A. Alexander-Katz, R. R. Netz, and M. F. Schneider, Proc. Natl. Acad. Sci. U.S.A. **104**, 7899 (2007).
[10] C. A. Siedlecki, B. J. Lestini, K. K. Kottke-Marchant, S. J. Eppell, D. L. Wilson, and R. E. Marchant, Blood **88**, 2939 (1996).
[11] A. Alexander-Katz, M. F. Schneider, S. W. Schneider, A. Wixforth, and R. R. Netz, Phys. Rev. Lett. **97**, 138101 (2006).
[12] H.-C. Yeh, Z. Zhou, H. Choi, S. Tekeoglu, W. May III, C. Wang, N. Turner, F. Scheiflinger, J. L. Moake, and J.-F. Dong, J. Thromb. Haemost. **8**, 2778 (2010).
[13] See Supplemental Material at http://link.aps.org/supplemental/10.1103/PhysRevLett.110.108102 for sample preparation and experimental methods.
[14] M. Rief, M. Gautel, F. Oesterhelt, J. M. Fernandez, and H. E. Gaub, Science **276**, 1109 (1997).

[15] P. E. Marszalek, H. Lu, H. Li, M. Carrion-Vazquez, A. F. Oberhauser, K. Schulten, and J. M. Fernandez, Nature (London) **402**, 100 (1999).
[16] M. Carrion-Vazquez, A. F. Oberhauser, S. B. Fowler, P. E. Marszalek, S. E. Broedel, J. Clarke, and J. M. Fernandez, Proc. Natl. Acad. Sci. U.S.A. **96**, 3694 (1999).
[17] N. C. Harris, Y. Song, and C.-H. Kiang, Phys. Rev. Lett. **99**, 068101 (2007).
[18] N. C. Harris and C.-H. Kiang, Phys. Rev. E **79**, 041912 (2009).
[19] F. Oesterhelt, D. Oesterhelt, M. Pfeiffer, A. Engel, H. E. Gaub, and D. J. Müller, Science **288**, 143 (2000).
[20] J. L. Moake, N. A. Turner, N. A. Stathopoulos, L. H. Nolasco, and J. D. Hellums, J. Clin. Invest. **78**, 1456 (1986).
[21] C. Baldauf, R. Schneppenheim, W. Stacklies, T. Obser, A. Pienconka, S. Schneppenheim, U. Budde, J. Zhou, and F. Gräter, J. Thromb. Haemost. **7**, 2096 (2009).
[22] A. J. Jakobi, A. Mashaghi, S. J. Tans, and E. G. Huizinga, Nat. Commun. **2**, 385 (2011).
[23] T. Wu, J. Lin, M. A. Cruz, J.-F. Dong, and C. Zhu, Blood **115**, 370 (2010).
[24] M. F. Iozzi, T. Helgaker, and E. Uggerud, J. Phys. Chem. A **115**, 2308 (2011).
[25] J. Ying, Y. Ling, L. A. Westfield, J. E. Sadler, and J.-Y. Shao, Biophys. J. **98**, 1685 (2010).
[26] I. Popa, J. M. Fernández, and S. Garcia-Manyes, J. Biol. Chem. **286**, 31 072 (2011).
[27] M. Mickler, M. Hessling, C. Ratzke, J. Buchner, and T. Hugel, Nat. Struct. Mol. Biol. **16**, 281 (2009).
[28] W. Y. Yang and M. Gruebele, Nature (London) **423**, 193 (2003).
[29] J. N. Onuchic, Z. Luthey-Schulten, and P. G. Wolynes, Annu. Rev. Phys. Chem. **48**, 545 (1997).
[30] J. Gore, Z. Bryant, M. D. Stone, M. Nöllmann, N. R. Cozzarelli, and C. Bustamante, Nature (London) **439**, 100 (2006).
[31] A. Šali, E. Shakhnovich, and M. Karplus, Nature (London) **369**, 248 (1994).
[32] G. J. L. Wuite, S. B. Smith, M. Young, D. Keller, and C. Bustamante, Nature (London) **404**, 103 (2000).
[33] C. Bustamante, J. F. Marko, E. D. Siggia, and S. Smith, Science **265**, 1599 (1994).
[34] B. Onoa, S. Dumont, J. Liphardt, S. B. Smith, I. Tinoco, Jr., and C. Bustamante, Science **299**, 1892 (2003).
[35] O. B. Bakajin, T. A. J. Duke, C. F. Chou, S. S. Chan, R. H. Austin, and E. C. Cox, Phys. Rev. Lett. **80**, 2737 (1998).